Volume 9, Number 10
1009-1963/2000/09(10)/0767-07
CHINESE PHYSICS
October, 2000
© 2000 Chin. Phys. Soc.

LOW TEMPERATURE OPTICAL PROPERTIES OF AMORPHOUS OXIDE NANOCLUSTERS IN POLYMETHYL METHACRYLATE MATRIX

V. V. Volkov[a], Wang Zhong-lin(王中林)[b], Zou Bing-suo(邹炳锁)[a,c,†], and Xie Si-shen(解思深)[c]

[a] *School of Chemistry and Biochemistry, Georgia Institute of Technology Atlanta, G. A.* 30332

[b] *School of Materials Science and Engineering, Georgia Institute of Technology Atlanta, G. A.* 30332

[c] *Institute of Physics, Chinese Academy of Sciences, Beijing* 100080, *China*

(Received 2 March 2000; revised manuscript received 30 May 2000)

We studied the temperature-dependent steady-state and time-resolved fluorescence properties of very small (1–2 nm) ZnO, CdO, and PbO amorphous nanoclusters prepared in AOT reverse micelles and imbedded in polymethyl methacrylate(PMMA) films. X-ray diffraction and electron diffraction and imaging indicate that these structures are amorphous. These amorphous oxide nanoclusters demonstrate similar structural, electronic, and optical properties. Properties of steady-state fluorescence spectra indicate the unique localization of electronic states due to the amorphous structure. ZnO and CdO show double-band fluorescence structure, which is due to the spin-orbital splitting, similar to Cu_2O. Time-resolved fluorescence studies of the nanoclusters in the polymer reveal two lifetime components, as found in solution. The slow component reflects relaxation processes from band-tail states while the fast component may be related to high-lying extended states. The temperature dependence of fast fluorescence component reveals the presence of exciton hopping between anharmonic wells at temperatures higher than 200K. We correlate the barrier height between two wells formed around local atoms with the inter-atomic distance and bond ionicity.

Keywords: nanocluster, optical properties, amorphous solids
PACC: 6295, 6278, 6154

I. INTRODUCTION

Since the first success in quantum confinement of electron (hole) wave functions, attention of the scientific community has been attracted to the manipulation of the optical properties of systems with reduced dimensions. Among others, II-VI semiconductor nanosystems are commonly investigated. The electronic properties of crystalline Cd, Zn, and Hg sulfides, selendides as related quantum dots, shells, and wells may not be completely understood although they have been extensively studied.[1–5] Several reports on crystalline ZnO-nanoparticle photochemical and optical properties have been published during last decade,[6–8] but the properties of amorphous oxide nanoclusters are out of traditional research interest. This is reasonable due to the complication in characterization of prepared systems. In many cases, reliability and validity of experimental results depend on the experience and expertise of whoever performed the synthesis. Some works have been recently published on quantum-confined states and the influence of surface states on the electronic structure of oxide nanoparticles.[9,10] Reported results indicate that oxide nanoparticles may have different optical properties from those of the II-VI semiconductor nanoparticles.

The packing limit of CdO and PbO, which form rock salt and rock-salt-like oxide nanoclusters consisting of several tens of metal ions, is determined by an octahedron of six oxygen atoms around a metal ion.[11] In contrast, ZnO nanoclusters have a wurtzite structure. Upon proper thermal treatment, ZnO nanoclusters (about 1–2 nm), coated with ionic surfactants, may undergo a transformation to the rock-salt-like nanostructures with similar absorption spectra (similar band gaps) to those of the CdO and PbO nanoclusters.

The results of our studies on the optical properties of very small (about 1–2 nm) amorphous nanoclusters of CdO, PbO, ZnO and thermally restructured ZnO in solution were discussed recently.[12] The similarity in UV-visible absorption and photoluminescence steady-state spectra of the ZnO, CdO and PbO nanocluster at room temperature reflects the similarity of their packing lattices and electronic structures. The optical properties of these materials suggest strong localization of the electronic excitation due to the amorphous

†Corresponding author.

structure and the surface coating. The time-resolved photoluminescence just near their band-tail demonstrates the picosecond and nanosecond components. This is different from that in the bulk amorphous semiconductor. It is clear that the extreme reduction of size, the strong electron-phonon coupling and the structural instability (leading to amorphization) distinguish this group of materials from any others.

Also, due to the specificity of the microemulsion method in preparing such materials in solution, their surface state may play an important role in determining the optical responses in these systems. Particularly, as in our case, a layer of anionic surfactants on the surface, serves for the protection of clusters from condensation and agglomeration in general, and also applies larger Coulomb potential on the material, thus altering the electronic structure and the optical properties.

In this work we continue the investigation on the optical properties of ZnO, CdO and PbO amorphous nanoclusters prepared in AOT reverse micelles. In order to examine the surface contribution and investigate the carrier dynamics, we incorporate our nanoclusters into the PMMA polymer matrix and study the absorption, the emission features, and the carrier lifetimes in quantum-confined states at temperatures in the range from 9 to 300 K. Low temperature studies of the ZnO, CdO, and PbO amorphous nanocluster optical properties in PMMA matrix reveal new spectral and dynamical features, consideration of which may help us in understanding of the electronic processes in amorphous nanoclusters.

II. EXPERIMENTAL

The ZnO, CdO, and PbO nanoclusters were prepared with the microemulsion method described in Ref.[12]. They are easily dispersed in chloroform. The PMMA films on quartz plates were prepared by mixing these organosols (5%) with the PMMA(95%) chloroform solution. So the nanoclusters stayed in polymer with no aggregation. The use of PMMA as a matrix is due to their transparency in the visible region. The nanoclusters were also proved to be 1–2 nm by dark-field transmission electron microscopy (TEM) observation as given in detail in Refs.[12] and [13].

Low temperature steady-state and time-resolved fluorescence measurements on the nanoclusters incorporated in the polymer matrix were performed with a closed-cycle refrigerator system, Janis CCS-150, operated between 10 to 325K. At least forty minutes settlement time for the temperature stabilization is needed before any data collection at each temperature.

A Beckman DU-650 spectrophotometer was used to measure the absorption spectra. The photoluminescence spectra of the ZnO, CdO, PbO nanoclusters in the reverse micelle were recorded using the PTI QM-1 and RC-M fluorescence systems.

The temporal behavior of the emission from the nanoclusters was measured using the time-correlated photon counting technique. The excitation source was 580 nm from a dye laser (Spectra-Physics, model 375B) with a cavity dumper. The dye laser was synchronously pumped by a mode-locked Nd:YAG laser (Spectra-Physics, model 3800). The pulse width was measured using an autocorrelator and was found to be 35 ps. The detection system was a microchannel plate photomultiplier tube (Hamamatsu R1564) coupled with a pulse-to-height converter (ORTEC, model 457), which provided an instrument response function of 40–60 ps (FWHM). The fluorescence decay was collected until 4000 counts were reached.

III. RESULTS AND DISCUSSION

A dark-field image recorded using the method introduced above was given in Ref[12]. The nanoclusters exhibited bright contrast and their size was measured to be 1–2 nm.

The indirect bandgap CdO(r.s.) and PbO(r.s.) are labeled as (r.s.) due to their rock salt and rock-salt-like structures respectively. The ZnO nanoclusters have wurtzite structure originally, but may have the rock-salt structure upon thermal treatment.[12] We prepared two samples of ZnO: ZnO(1) was thermal-treated at 475 K, below which the ZnO nanocluster solution was colorless and transparent; ZnO(2) was obtained under thermal treatment at higher temperatures (550–600 K), which led to longer wavelength absorption and related smaller band gap. The X-ray diffraction and the electron diffraction techniques indicated that all our samples were amorphous.[14,15] The absorption spectra(a) and related electronic structure(b) of the ZnO(1), CdO(r.s.), PbO(r.s.) and ZnO(2) nanoclusters in the reverse micelle in solution at room temperature are given in Fig.1. We found the band-edge of the present samples to be around 580 nm for ZnO(1), 600 nm for CdO, 650 nm for PbO, and 700 nm for ZnO(2) using Tauc's band-edge model from the indirect equation $(\alpha h\omega)^{3/2} = A(h\omega - E_g)$.[12] A weak tail in the absorption below the direct band

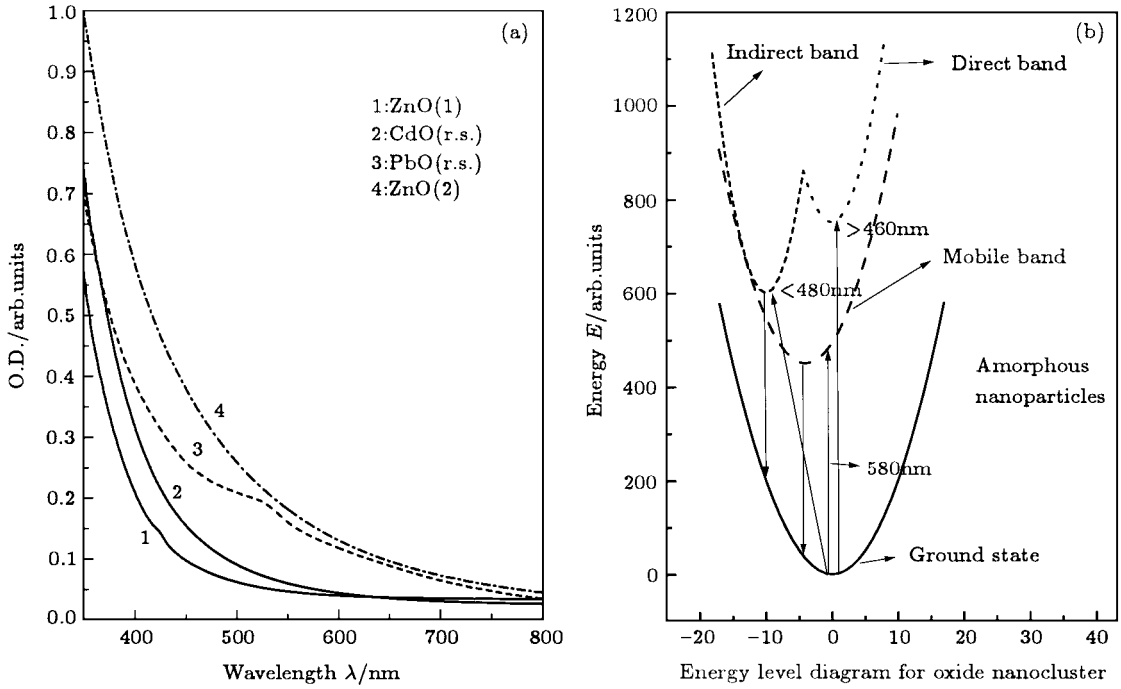


Fig.1. Absorption spectra(a) and electronic structure of unit cell (b)[12] for ZnO(1), CdO(r.s.), PbO(r.s.) and ZnO(2) amorphous nanoclusters at room temperature. CdO(r.s.) and PbO(r.s.) are labeled due to their rock salt and rock-salt-like structures respectively. ZnO(1) is thermal-treated at 475 K, ZnO(2) is obtained under thermal-treatment at higher temperature(550–600 K), the ground state is composed of two valence band due to spin-orbital splitting..

suggests the presence of in-gap density of states, due to the structural disorder.

The strong confinement, together with the structural disorder, modulates and even breaks down the zone structure and forms an ensemble of anharmonic oscillators. Such a reorganization of the electronic structure occurs in the presence of the strong surface polarization. These factors not only explain the observed bandedge red-shifted character, but also can justify the good fluorescence efficiency resulting from the direct-transition-like character in our nanosystems,[12] while the related bulk materials are optically silent, indirect semiconductors.

The steady-state fluorescence spectra of the ZnO, CdO, PbO nanoclusters in reverse micelles recorded at 400, 468 and 500 nm excitations at 10 K are given in Fig.2. First of all, there is a unique similarity in the optical responses from all of our compounds. The emission bands appear to be broad even at 10 K, especially for the PbO cluster which is different from ZnO and CdO, since the latter two have a structured emission band. This difference cannot be observed at room temperature. The fluorescence depends on the excitation wavelength and the emission maximum is clearly Stokes-shifted. If the excitation lines are close to the bandedge of these nanomaterials, the values of the respective Stokes-shifts decrease slightly with long wavelength excitation.

Another striking feature of the fluorescence is the notable double-band character at low temperature. Figures 3 and 4 demonstrate the disappearance of this feature upon heating, for CdO and ZnO(2) clusters from 10 to 300 K. For bulk material, we should consider the two series of conduction bands from 400 to 600 nm due to the crystal-field splitting of the metal ions. The first one is from the direct transition in the spectral region around 400–480 nm; the second one is from the indirect transition of around 480–600 nm. Both of the above bands contain two components(subband), due to the spin-orbital splitting of the oxygen valence band(at an energy of around 1000 cm^{-1}). In Figs.3 and 4 one can see this spin-orbital splitting. Under excitation with photon energy less than 2.25 eV (wavelength around 550 nm), the emission may come from the in-gap states or mobile gap states (due to the amorphous structure), which become possible due to the surface-assisted or the disorder-induced carrier localization, i.e., not an intrinsic band. If this is the case, then the observed fluorescence double-band structure represents the same

upper energy level as the levels of spin-orbital splitting in the oxygen valence band, which is present in the close-packed oxygen structure in metal oxides. The spin-orbital splitting is a little larger if the system is excited with longer wavelength. In reality this doublet reflects the MO_6 octahedral in these nanoclusters.[9] However, There is no obvious double-band character for the PbO. The large ions like PbO_6 show no such structure in the emission band because Pb-O bond has larger polarizability and strong mixing between $Pb7s^2$ and oxygen O2p orbitals in the valence band of PbO.

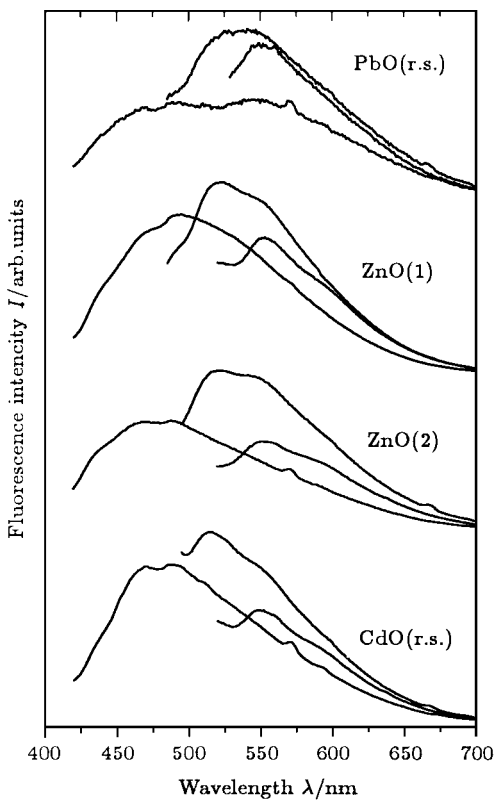


Fig.2. Emission spectra for ZnO(1), CdO, PbO and ZnO(2) amorphous nanoclusters in PMMA matrix at 400, 468, and 500 nm excitations recorded at 10 K.

It is clear from the spectral profiles (Figs.2–4) that CdO and ZnO are very similar. This is because they belong to the same column in the Periodic Table. For example, CdO and ZnO have the same profile of fluorescence at 468 and 500 nm excitations (Figs.3 and 4). Their fluorescence intensities under 468 nm excitation are about twice those under 500 nm excitation. This is because the 468nm excitation promotes the electrons to the direct band, while 500 nm excites the electrons to the indirect band. In contrast, the fluorescence intensities for the PbO under 468 and 500 nm excitations are comparable due to strong band-mixing, indicating that the indirect and direct bands in PbO nanoclusters cannot be distinguished from each other. Another cause may be that the direct band edge is at around 520 nm in PbO nanocluster obtained from the absorption spectra, which is much lower than that in ZnO and CdO of 460 nm.

We observe that the emission intensity increase as temperature decreases for all samples (Figs.3 and 4). The dependence of relative fluorescence efficiency on temperature is given in Fig.5. The dependence has a complicated character, which was theoretically explained by Henglein *et al.*[16] There is an insensitive region in the low temperature range. The width of this insensitive range reflects the extent of carrier delocalization. The higher the temperature for fluorescence intensity keeping unchanged, the more the carrier delocalization and the smaller the carrier mass, so generally the smaller the bandgap of nanoparticles. The fluorescence intensities do not change much as temperature increases to 100 K. They even slightly increase around 150 K for PbO and ZnO(2) clusters. This is in agreement with their smaller bandgap. The flat part is followed by the clear decay of fluorescence intensity with increasing temperature. The ZnO(1) and CdO

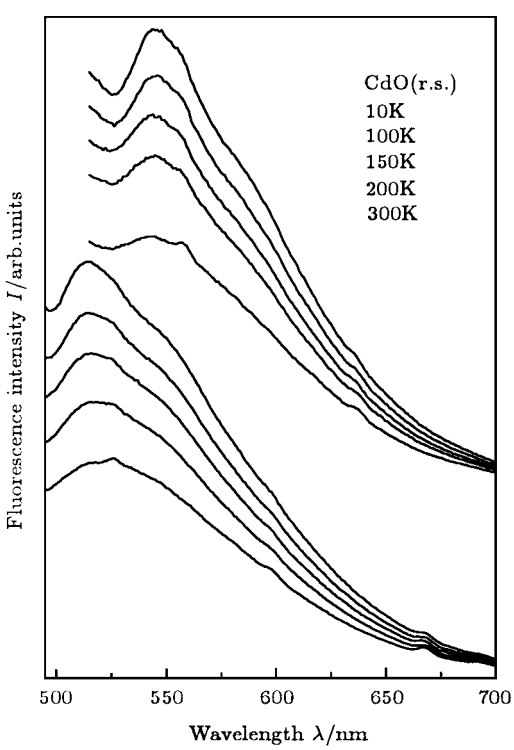


Fig.3. Emission spectra for CdO (rock-salt) amorphous nanoclusters in PMMA matrix at 468, and 500 nm excitations recorded at 10, 100, 150, 200, 300 K (the higher the temperature, the lower the intensity of emission).

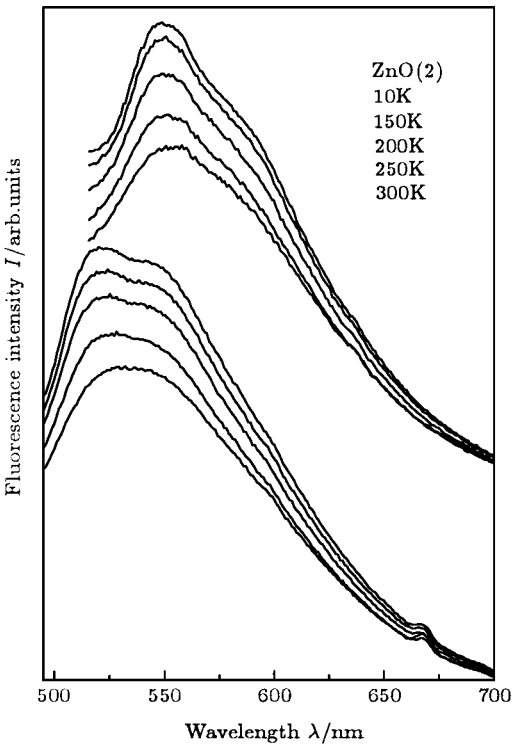


Fig.4. Emission spectra for ZnO(2) amorphous nanoclusters in PMMA matrix at 468, and 500 nm excitations recorded at 10, 150, 200, 250, 300K (the higher the temperature, the lower the intensity of emission).

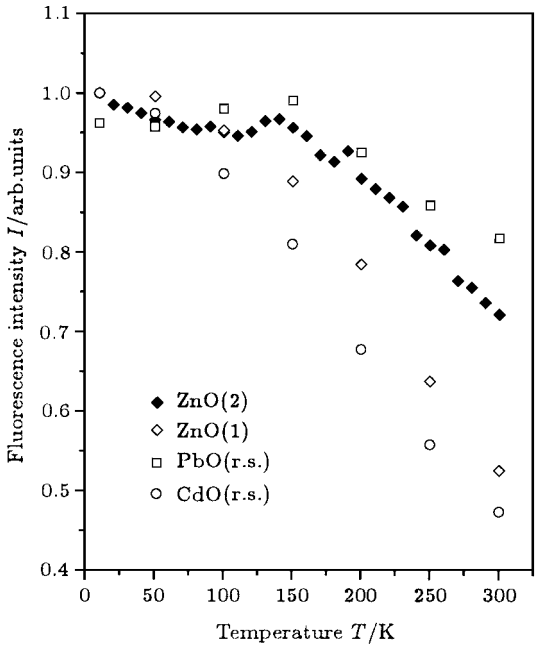


Fig.5. Relative fluorescence efficiency for ZnO(1), CdO, PbO and ZnO(2) amorphous nanoclusters in PMMA matrix depending on temperature (estimated for the 500 nm excitation experiments).

fluorescence efficiencies turn out to be temperature-dependent in a much lower temperature range. Such a behavior is definitely determined by the effective carrier mass and the characteristic energy of lattice vibrations in our systems, due to the successful freezing of the phonon modes participating in the non-radiative relaxation processes.[17]

The time-resolved fluorescence studies with 580 nm excitation on the ZnO (1), CdO, PbO, ZnO (2) clusters in polymer reveal two lifetime components, as those seen in solution. The fast one is in the range of 300–700 ps; the slow one varies from 3 to 4 ns, depending on the kind of sample. The slow component reflects the relaxation processes from the band-tail states, while the fast component may be related to the high-lying extended states. The lifetimes of the CdO, PbO and ZnO(2) (not of ZnO(1)) nanoclusters in PMMA film at low temperatures are about 200 ps longer than the corresponding ones in toluene at room temperature(see Table 1). This is a result of the reduction of thermal relaxation and phonon scattering. At room temperature the lifetimes are also longer than those in solution. It is important to notice these observed differences of carrier lifetimes in these nanoclusters. Now we are restricted to the consideration of the surface/solvent related factors.

Table 1. Fluorescence life-times (τ_1 and τ_2) for ZnO(1), CdO, PbO and ZnO(2) amorphous nanoclusters in PMMA matrix, and in toluene, at 580 nm excitation.

System	τ_1/ps and τ_2/ps in PMMA		τ_1/ps and τ_2/ns in toluene	
ZnO(1)	360,	3.0	600,	3.5
ZnO(2)	570,	3.3	130,	1.1
CdO(r.s.)	580,	3.35	360,	2.8
PbO(r.s.)	690,	3.80	270,	2.0

The motion and collisions of nanoclusters in solution may be important as in the case of molecular systems. From this point of view, the surface and the carrier mass should participate in the determination of relaxation times. Since the sizes of ZnO(1), ZnO(2), CdO and PbO clusters are the same (determined by the micelle), the only factor which may be correlated with the motion is the mass of the cluster. The heavier nanoparticle moves and transfers energy to the solvent slower and thus should have the longer excitation lifetime. Hence the decrease of the lifetime in the order of CdO, PbO in solution may be dictated not only by the values of the relative band gaps and the carrier mass but also by the cluster masses. However, in polymer the order of lifetimes of these nanoclusters correlates

well with the order of smaller band gap, i.e., the order of higher ionicity and larger polarization of ZnO, CdO, PbO. Because the ionicity of these similar rock salt nanostructures may change insignificantly, ionic polarization should play a dominant role in determining the band gap. So the highest polarization between lead and oxygen provides the lightest mass of carriers in our systems, hence the longest lifetime. Interestingly to notice that ZnO(2) has higher polarization on surface than ZnO(1), so it has a lifetime close to CdO, longer than ZnO(1). However, the longer lifetime of ZnO(1) in solution than in polymer could be due to the mobile band gap blue shift at lower temperatures, and 580 excitation at low temperatures can only excite the ingap state. From the above results we can see that the surface polarization can affect the band gap of nanoclusters, as well as the carrier mass and carrier-phonon interaction.

The fast-lifetime component of the ZnO, CdO, PbO nanoclusters in PMMA film increases as the temperature decreases down to 200K, and then it remains constant for all the systems. The lifetime of ZnO(1) clusters is almost temperature insensitive up to room temperature. Their Arrhenius plots can be drawn and the activation energies for the excitation relaxation in these nanocluster systems can be estimated(see Fig.6).

At this point it is necessary to return to the general consideration of the carrier dynamics in our systems. As we discussed earlier for the system with strong quantum confinement, where structural disorder breaks down the electronic structure to the ensemble of anharmonic oscillator potentials, the electronic states are mixed and the transition rules are relaxed. This provides the unprecedented basis of highly localized nature of excitations. Such localized excitation relaxes in its own well or migrates to the very proximal wells. As a result, we do not observe optical features typical for delocalized exciton migration to the low-lying shallow or deep traps in our systems, as that in II-VI semiconductor nanocrystals.[12] The localized exciton hopping from one well into another is associated with the thermal-assisted process overcoming an energy barrier, which is naturally formed by the independent potential wells. So the localized exciton gives a broad band as in Figs.2–4. In the higher temperature range the barrier hopping via phonon assistance can happen. With decreasing temperature, important lattice modes may eventually freeze out and thus energy relaxation will be determined by migration, which occurs by quantum tunneling predominantly, while those processes through the assistance of LO phonons or scattering of the lower acoustic phonons would decrease.

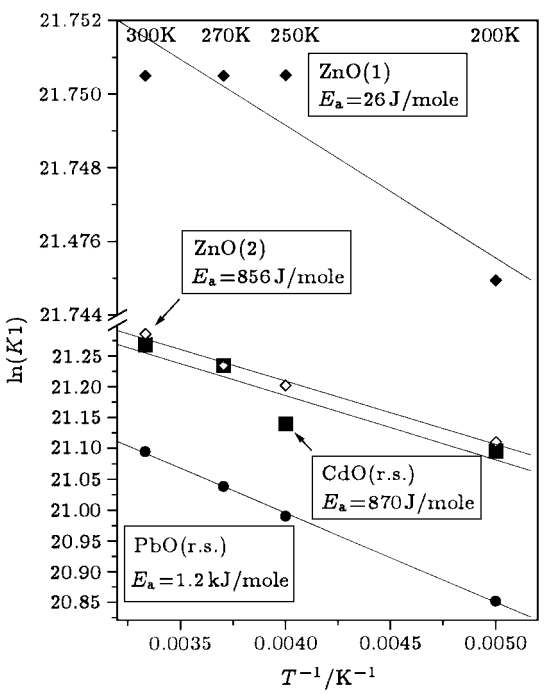


Fig.6. Arrhenius plots for ZnO(1), CdO, PbO and ZnO(2) amorphous nanoclusters in PMMA matrix.

The fast lifetime component at about 200 K and lower temperatures is found to be temperature independent for all the systems; 200 K corresponds to the 140 cm^{-1} phonon. This is highly related to metal component of LO mode and acoustic multi-modes of M-O bond vibration. As the height of the barrier between two wells, this energy reflects the strong potential fluctuations in the wells in nanoclusters. So the wide range of activation energies estimated for our systems (see Fig.6) may be rationalized in a simple way, as a result of the anharmonic surface minima of the displacement related to the interatomic distance. From this point of view the largest activation barrier for PbO is reasonable. Almost equal barrier heights for CdO and ZnO(2) imply the unprecedented similarities in their structure and electronic structures. The ZnO(1) is the one with the least barriers. It is not clear what kind of modification occurs with the wurtzite zinc oxide under the temperature treatment to differentiate the properties of ZnO(2) from that of the original system. The difference between ZnO(1) and ZnO(2) indicates the variation of the temperature effect on the structure and electronic states. This means that the degree of amorphization in ZnO(1) is not so high that the relaxation time is ruled by a zone-like structure and

the highly localized states are not dominant, i.e., one has a more complicated structure in ZnO(1). But in ZnO(2) a stronger surface polarization and a local-well state dominate. Finally, we would like to mention one more feature that supports our model. The values of Stokes shifts of these nanosystems correlate well with the barrier heights, and thus with the displacements of the anharmonic surface minima.

The relative fluorescence efficiency is helpful in further consideration of the lattice vibration contribution in the excitation relaxation of our system. As we suggested, there is less exciton hopping, but dominant tunneling upon lowering the temperatures below 200 K. This gives another support to the idea that the exciton should relax in its own well at temperature lower than 200 K. The emission band narrowing and the discrete bands are good evidences for that also. At temperatures lower than 200 K we deal mostly with pure relaxation within one well. Inspite of similarities in material structure and optical properties, the different temperature dependencies of the relative fluorescence efficiencies for our systems suggest that excitation scattering due to low frequency phonon modes ($<140\,\mathrm{cm}^{-1}$) is different for different compound in our samples. This is in agreement with our infrared spectra of ZnO(2).[15] These characteristicses reflect the degree of structure disorder and carrier localization in these nanosystems.

IV. CONCLUSION

Low temperature emission profiles of amorphous ZnO and CdO nanoclusters show clearer doublet structures than in solution,[12] which support that they have similar lattice and electronic states; however, PbO nanocluster show not clear doublet emission structure due to more band-mixing. The results of low temperature steady and transient photoluminescence of amorphous ZnO(1), ZnO(2), CdO, and PbO nanoclusters confirm the mobile band gap and localized transitions in these nanosystems. The spectroscopic behaviors of ZnO(1) and ZnO(2) reflect the disorder's influence on bandgap and relaxation. The emission band position change with excitation wavelength reflects the localized state nature in amorphous semiconductor; however, their lifetimes are several orders less than that in the bulk amorphous semiconductor. Their emission intensity changes with temperature, lifetime and activation energy of ZnO(1), CdO and PbO nanoclusters indicate that the relaxation is determined by the band gap, ion distance and the degree of disroder. This conclusion can not be obtained clearly from nanoclusters in solution, in which the nanocluster mass and nanocluster motion also play a role in the excited state relaxations. These results give a basic diagram of the electronic structures and excited state relaxation of the amorphous nanosized oxide, which are in contrast to the amorphous bulk-systems.

ACKNOWLEDGMENTS

We thank Professor M.A. El-Sayed for supplying the facility in carrying out the reported research and his encouragement. VVV, BSZ and ZLW thank the financial supports from the Office of Naval Research (Grant No. DE-FG03-88ER-13828), the Molecular Design Institute at Georgia Institute of Technology and NSF DMR-9733160, respectively.

REFERENCES

[1] N. Chestnoy, R. Hull, L. E. Brus, *J. Chem. Phys.*, **85**(1986), 2237.
[2] L. E. Brus, *J. Chem. Phys.*, **79**(1983),5566.
[3] L. E. Brus, *J. Chem. Phys.*, **80**(1984),4403.
[4] H. Temkin, G. Dolan, M. Panish, S.Chu, *Appl. Phys. Lett.*, **50**(1987),413.
[5] M. Reed, J. Randall, R. Aggarwal, R. Matyi, T. Moore, A. Wetsel, *Phys. Rev. Lett.*, **60**(1988),535.
[6] M. Haase, H. Weller, A.Henglein, *J. Phys. Chem.*, **92** (1988),482.
[7] P. V. Kamat, B. Patrick, *J. Phys. Chem.*, **96**(1992), 6829.
[8] J. J. Cavaleri, D. E. Skinner, D. P. Colombo, Jr., R. M. Bowman, *J. Chem. Phys.*, **103**(1995),5378.
[9] B. S. Zou, J. Lin, J. Xu, Q. Wei, L. Xiao, T. Li, *Physics of Low Dimensional Structures*, **1/2**(1996),173.
[10] R. Araujo, J. Butty, N. Peyghambarian, *Appl. Phys. Lett.*, **68**(1996),584.
[11] C. Vesley, D. Langer, *Phys. Rev.*, **B4**(1971),451.
[12] B. S. Zou, Z. L. Wang, V. V. Volkov, *Chem. Mater.*, **11**(1999),3037.
[13] Z. L. Wang, Elastic and Inelastic Scattering in Electron Diffraction and Imaging (Plenum Press,1995), Chaps. 1 and 6.
[14] B. S. Zou, G. Q. Tang, G. Zhang, W. Chen, *Acta Physica Sinica*, **44**(1995),164(in Chinese).
[15] B. S. Zou, B. Wang, W. Chen, *Chinese Science Bulletin*, **39**(6)(1994),499.
[16] A. Henglein, B. Bunsenges, *Phys. Chem.*, **86**(1982),301.
[17] K. Misawa, H. Yao, T. Hayashi, T. Kobayashi, *J. Lumi.*, **48 & 49**(1991),269.